A WALL INTERFERENCE ASSESSMENT/CORRECTION SYSTEM

SEMI-ANNUAL REPORT #4 JANUARY - JUNE 1993

Dr. C.F. Lo, Principal Investigator
University of Tennessee Space Institute

NASA Ames Research Center NAG 2-733

Ames Research Center
Moffett Field, CA 94035-1000

INSTITUTION:

CSTAR - Center for Space Transportation and Applied Research
UTSI Research Park
Tullahoma, TN 37388-8897

Phone 615-455-9294 or 5884

A WALL INTERFERENCE ASSESSMENT/CORRECTION SYSTEM

SEMI-ANNUAL
REPORT #4
JANUARY - JUNE 1993

Dr. C.F. Lo, Principal Investigator
University of Tennessee Space Institute

NASA Ames Research Center NAG 2-733

Ames Research Center
Moffett Field, CA 94035-1000

INSTITUTION:

CSTAR - Center for Space
Transportation and Applied Research
UTSI Research Park
Tullahoma, TN 37388-8897

Phone 615-455-9294 or 5884

Title: A Wall Interference Assessment/Correction System

Semi-Annual Report #4
January-June, 1993

Principal Investigator:
Dr. C. F. Lo, UTSI
Other Investigators
Mr. Glenn Overby, GRA/UTSI
Ms. Cathy X. Qian, GRA/UTSI
Mr. W. L. Sickles, CSTAR/Calspan

Technical Officer:
Dr. Frank W. Steinle, Jr. NASA/Ames Research Center

Technical Objectives

A Wall Signature method originally developed by Hackett has been selected to be adapted for the Ames 12-ft Wind Tunnel WIAC system in the project. This method uses limited measurements of the static pressure at the wall, in conjunction with the solid wall boundary condition, to determine the strength and distribution of singularities representing the test article. The singularities are used in turn for estimating wall interference at the model location. The lifting interference will be treated separately by representing in a horseshoe vortex system for the model's lifting effects. The development and implementation of a working prototype will be completed, delivered and documented with a software manual.

The WIAC code will be validated by conducting numerically simulated experiments rather actual wind tunnel experiments. The simulations will be used to generate both free-air and confined wind-tunnel flow fields for each of the test articles over a range of test configurations. Specifically, the pressure signature at the test section wall will be computed for the tunnel case to provide the simulated "measured" data. These data will serve as the input for the WIAC method--Wall Signature method. The performance of the WIAC method then may be evaluated by comparing the corrected parameters with those for the free-air simulation.

The following two additional tasks are included in the supplement No. 1 to the basic Grant. (1) On-line wall interference calculation: The developed wall signature method (modified Hackett's method) for Ames 12-ft Tunnel will be the pre-computed coefficients which facilitate the on-line calculation of wall interference. and (2) Support system effects estimation: The effects on the wall pressure measurements due to the presence of the model support systems will be evaluated.

Status of Progress

A. Wall Signature Method

The Wall Signature method was investigated to calculate the blockage correction in the NASA/ARC 12-ft Pressure Wind Tunnel. The blockage correction which was developed and implemented for a rectangular tunnel as well as the 12-ft Pressure Tunnel is reported in Ulbrich's Ph.D. dissertation. (Ref. 1).

B. Support Systems Interference

The effort of this period is concentrated at the effect of the model support system in the 12-ft Pressure Tunnel on the tunnel wall pressure signature measurements. The study has also been investigated by the PMARC code (Ref. 2). Since the Wall Signature method is based upon the wall pressure measurement to estimate the wall interference. The consideration of the effects of the support systems on the wall pressure is critical and essential to accurately assure the wall pressure only induced by wall interference and model effects. Therefore, the study of support systems interference is required to estimate the amount of effects due to the support system. The result is summarized in a CSTAR technical report which is attached in Appendix I.

Future Plan:

The development of the lifting correction of Wall signature method will continue. It will be incorporated into the overall interference correction calculation. The NACA 4412 airfoil is a candidate for continuing the investigation of lifting and blockage interferences together in the future periods.

References:

1. Ulbrich, N., "Wall Interference Correction Based on Interface Measurements in Subsonic Wind Tunnel Testing," Ph. D. dissertation, The University of Tennessee, Knoxville, TN, August 1992.

2. Ashby, D. L., Dudley, M. R., Iguchi, S. K., Browne, L., Katz, J., "Potential Flow Theory and Operation Guide for the Panel Code PMARC," NASA TM 102851, NASA Ames Research Center, Moffett Field, California, January 1991.

APPENDIX I

SUPPORT SYSTEM INTERFERENCE STUDY FOR THE NASA/ARC 12-FT PRESSURE WIND TUNNEL

Glenn Overbey
and
Ching F. Lo

The University of Tennessee Space Institute

May 1993

The University of Tennessee-Calspan
Center for Space Transportation & Applied Research
UTSI Research Park
Tullahoma TN 37388-8897
(615) 454-9294 FAX: (615) 455-6167

Preface

This work was supported under NASA Ames Research Center NAG 2-733. The technical officer for this grant is Dr. Frank W. Steinle, Jr., Aerodynamics Facility Branch, 227-5, NASA/ARC, Moffett Field, CA 94036. Most of this document was reported as the first author's thesis for a Master of Science degree in Aerospace Engineering at the University of Tennessee Space Institute.

We would like to express our thanks to the staff of the Center for Space Transportation and Applied Research (CSTAR) for providing the computer facilities needed for this investigation. Our sincere gratitude is also extended to Dr. George Shi and Dr. Norbert Ulbrich for their help in learning the panel method code, PMARC.

Summary

A study was conducted in order to determine the support system interference on the wall pressures in the NASA Ames 12 foot pressure wind tunnel. The influence of the support system on the wall pressures must be determined in order to accurately correct for blockage and lift effects due to the presence of the walls. A panel method code, PMARC, was used to determine if the support system, consisting of a strut and sting and a bi-pod type support, influenced the static pressure measurements at the wall of the tunnel near the model position.

The NACA 4412 airfoil was used to examine the accuracy of the code. A two-dimensional case was compared with results from another panel code, VSAERO. A three-dimensional case was compared with published data for this airfoil. The results from these calculations agreed with published data obtained both with another panel code and from actual experiments.

Inviscid theory was used to explain a velocity spike encountered at the entrance to the diffuser. The calculations were performed for two different sizes of a model attached to the strut and sting support. An analysis was performed to determine the effect of the presence of a wake from the bi-pod support on the wall pressures. A model was not used in conjunction with the bi-pod support.

The results of this investigation show that the sting and strut support system does not influence the static pressures measured along the wall around the model location. The bi-pod support was shown to have a larger influence on the wall static pressures due to the fact that it is located directly under the model.

Table of Contents

List of Figures

Nomenclature

B_{jk}	Velocity potential influence coefficient per unit source strength for panel k acting on the control point of panel j
C_{jk}	Velocity potential influence coefficient per unit doublet strength for panel k acting on the control point of panel j
$\hat{n}$	Unit vector normal to the surface
r	Distance from a surface element to a point in the region of interest
S	Total surface boundary over which the surface integral is taken
$\overline{V}$	Relative velocity between the body and the fluid
V_{norm}	Normal velocity on the surface
$\overline{V}_{\infty}$	Free-stream velocity vector
v_r	Radial velocity component
v_θ	Angular velocity component
α	Corner angle
α_0	Effective angle of attack
μ	Doublet
Φ	Velocity potential of the flow of interest
Φ_P	Velocity potential at any point in the flow
Φ_{∞}	Free-stream velocity potential
σ	Source

1.0 Introduction

The wall pressure signature method as described by Hackett and Wilsden (1), Kemp (2), Ashill and Weeks (3), and Ulbrich et al. (4), and other recently developed methods such as that described by Lo (5), use static pressure measurements to estimate the wall interference in a wind tunnel test. The interference of the support systems on the wall pressure must be considered when attempting to determine the wall interferences on the model based on the wall pressure measurements. If the support system is causing a change in the wall pressure near the location of the model, then this must be taken into account when the corrections to the test data are applied. Therefore, an investigation of the model support system interference on the wall pressure is required for the renovated 12 foot Pressure Wind Tunnel at NASA Ames Research Center.

1.1 Objectives

NASA Ames Research Center is renovating the 12 foot Pressure Wind Tunnel. The renovation involves the development of two supports; the strut and sting support and the bi-pod support. The purpose of this investigation is to determine the effect of these two support systems on the wall pressures near the model location. The wall pressure signature method is used to determine the wall interference on the test results. This process involves measuring the static pressure at the walls of the tunnel and using these measurements to correct for blockage and lift effects due to the model and the walls. Therefore, the influence of the support system on the wall pressure must be determined to ensure that the effects at the walls are due only to the presence of the model and the walls themselves.

1.2 Low Order Panel Method Codes

A low order panel method code was selected for this investigation for several reasons. First, a low order code does not require the huge amounts of computation time that a higher order code would require. This is due to the fact that low order panel methods distribute the singularities with constant strength over the panels, whereas high order panel methods allow the singularity strengths to vary over each panel. While high order panel methods provide better accuracy, low order methods can produce almost the same level of accuracy as higher order methods without requiring lengthy computation times (6).

1.3 PMARC Selection

PMARC (Panel Method Ames Research Center) can be used on various machines from a Macintosh II workstation to a Cray Y-MP (6). Also, PMARC is an adjustable size panel code which allows the code to be customized to a particular user's system. Most of the computations for this investigation were done on an IBM RISC 6000 machine although some of the preliminary calculations were done on a desktop PC-486 machine.

Since the wind tunnel of this investigation is a subsonic tunnel, PMARC was an excellent choice for the panel code to be used. It was flexible enough to be able to handle all of the cases from a simple rectangular wing in free air to a complete model and support system within a wind tunnel. PMARC has the ability to model complex geometries consisting of many different components with a minimum of time required to enter the geometry description.

1.4 Approach

Preliminary calculations were performed on the NACA 4412 airfoil to validate the results since experimental data for this airfoil was readily available (7). These preliminary calculations consisted of both two-dimensional airfoil cases and three-dimensional wing cases. For the two-dimensional case, the results of the calculations were compared to the results from another panel code, VSAERO (8). The three-dimensional wing results were compared to experimental wind tunnel data obtained by Pinkerton (7).

An analysis, based on inviscid theory, of the effect on the wall pressures of the diverging walls at the end of the tunnel test section was performed. This was done to explain the pressure peaks encountered at the beginning of the diffuser. Since the strut support was located in this section of the tunnel, the effect of this strut had to be separated from the effect of corner flow from inviscid theory, which predicts that the velocity at a corner will increase. Such an analysis also served to verify the results obtained with PMARC.

A NACA model (9) was used as the test model for this investigation. This model consisted of a wing of 45° sweepback attached to a pointed circular cylindrical body. This model was chosen because of its simple geometry and to be able to compare the results with previous studies of this tunnel with PMARC. Two different sizes of this model were used to determine if a larger model with a shorter sting produced different effects on the wall static pressures.

2.0 Theory and Background

The basic potential flow problem is based on an irrotational, incompressible flow. From continuity for such a flow, Laplace's equation is developed.

$$\nabla^2\Phi = 0 \tag{2.1}$$

In order to solve the potential flow problem, boundary conditions must be specified. The first boundary condition is that there is no flow through the body surface as given by Equation (2.2).

$$\nabla\Phi \cdot \hat{n} = 0 \tag{2.2}$$

The vector normal to the surface is represented by $\hat{n}$ and points outside the region of interest.

The second boundary condition is that the disturbance due to the body decays far from the body (i.e. as $r \rightarrow \infty$). This condition can be stated as:

$$\lim_{r\to\infty}\left(\nabla\Phi - \overline{V}\right) = 0 \tag{2.3}$$

where $\overline{V}$ is the relative velocity between the body and the fluid.

Ashby et al. (6) defines the source as

$$4\pi\sigma = -\hat{n}\cdot\left(\nabla\Phi - \nabla\Phi_\infty\right) \tag{2.4}$$

where $\hat{n}$ now points into the flow field of interest. Based on Equation (2.4), the source strengths can be solved for directly if the normal velocity at the surface is assumed to be zero or some known value. Equation (2.5) gives the source strengths on the surface.

$$\sigma = \frac{1}{4\pi}\left(V_{norm} - \hat{n}\cdot\overline{V}_\infty\right) \tag{2.5}$$

Since the freestream velocity, $\overline{V}_\infty$, is known and the normal velocity is zero (for a solid boundary) or a user defined value (for a suction or blowing surface), the source strengths are thus determined.

Ashby et al. (6) then derives an equation for the potential at any point P as

$$\Phi_P = \left[\iint_{S-P} \mu \hat{n} \cdot \nabla\left(\frac{1}{r}\right) dS + K\mu_P \right] + \iint_S \left(\frac{\sigma}{r}\right) dS + \iint_W \mu_W \hat{n} \cdot \nabla\left(\frac{1}{r}\right) dS + \Phi_{\infty_P} \qquad (2.6)$$

where: K = 0 if P is not on the surface
K = 2π if P is on a smooth part of the outer surface
K = -2π if P is on a smooth part of the inner surface
K = the solid angle contained at the crease if P lies at a crease in the surface

To apply the above equations to a panel method, the surface geometry must be divided into panels. Equation (2.6) can be written in discretized form such that the integrals are broken up into surface integrals over each panel. PMARC is a low order panel method and, therefore, it assumes a constant strength source and doublet distribution over each panel. These constant source and doublet strengths can be factored out of the integrals.

The point P is taken to be at the centroid on the inside surface of one of the panels. The surface integrals over each panel are then summed for all panels. If the panel contains P, the surface integral is zero and only the $-2\pi\mu_p$ term remains in the bracketed part of Equation (2.6). For all other panels, the $-2\pi\mu_p$ term is zero since P is not on the surface of any of the other panels and the surface integral is used. This process is repeated for each panel and results in a set of linear simultaneous equations to be solved for the unknown doublet strength on each panel (6). Therefore, Equation (2.6) can be written as

$$\sum_{k=1}^{N_S} (\mu_k C_{jk}) + \sum_{k=1}^{N_S} (\sigma_k B_{jk}) + \sum_{l=1}^{N_W} (\mu_{W_l} C_{jl}) = 0 \Big|_{j=1,N_S} \qquad (2.7)$$

where

$$B_{jk} = \iint_k \frac{1}{r} dS \qquad (2.8)$$

and

$$C_{jk} = \iint_k \hat{n} \cdot \nabla\left(\frac{1}{r}\right) dS$$
$$C_{jj} = -2\pi \qquad (2.9)$$

These values, B_{jk} and C_{jk}, represent the velocity potential influence coefficients per unit singularity strength for panel k acting on the control point of panel j. Equations (2.8) and (2.9) are functions of geometry only and can be solved for all panels to form the influence coefficient matrix (6).

2.1 Verification

In order to become familiar with a code as complex as PMARC, it is necessary to use it to calculate cases for which data is available. The NACA 4412 airfoil was chosen as the test article because experimental data was readily available for this airfoil. This airfoil had also been used in previous studies which were based on VSAERO, a panel code that was the basis for the development of PMARC (8).

2.1.1 Two-Dimensional Airfoil

The goal of this first set of calculations was to reproduce the two-dimensional airfoil data obtained with VSAERO (8) by using PMARC. A wing was modeled using the NACA 4412 airfoil with a chord of 1 foot and a span of 20 feet (aspect ratio of 20). The wing was modeled with five panels in the chordwise direction over the first 10% of the chord using half cosine spacing and 12 panels equally spaced over the remaining 90% of the chord for both the upper and lower surface. There were 12 panels in the spanwise direction for a total of 408 panels on the wing surface.

This wing was placed in a large rectangular wind tunnel (20 ft. x 20 ft. x 40 ft.). By extending the wing to the walls of the tunnel and using the data near the centerline, a reasonable approximation of the two-dimensional airfoil results should have been obtained. The wing was set at an angle of attack of zero degrees. A wake was defined from the trailing edge to a point in the stream ten chord lengths from the trailing edge of the wing. Time stepping of the wake was not used for this case. The pressure coefficients, as calculated by PMARC and compared with results from VSAERO, for both the upper and lower surface near the centerline are shown in Figure 2.1. These results indicate a good agreement on the aft 60% of the chord for the two-dimensional airfoil case between Ashby and Sandlin's published data (8) and this investigation. PMARC tended to over-predict the pressure coefficient near the leading edge of the airfoil particularly on the upper surface. There is approximately a 12% difference between Ashby and Sandlin's (8) results and those obtained with PMARC from the 20% to 40% chord position. This discrepancy is explained by the difference in solid blockage for these two investigations.

Ashby and Sandlin's (8) calculations were performed for a 7 x 10 foot tunnel, however, they did not report the dimensions of their wing. Since Ashby and Sandlin's tunnel is less than half the size of the test section used in this investigation, the solid blockage they experienced is probably considerably greater than that encountered in this investigation (0.6%). The blockage of Ashby and Sandlin's test was estimated to be on the order of 5% by examining the geometry of their test. As the solid blockage increases, the velocity around the model increases which results in a decrease in the local pressure and thus a decrease in the pressure coefficient. Therefore, larger solid blockage would account for the lower pressure coefficients over the upper surface of the wing obtained by Ashby and Sandlin as compared to those calculated for this investigation.

2.1.2 Three-Dimensional Wing

The next step was to attempt to model a three-dimensional wing using PMARC. The wing was modeled similarly to the two-dimensional case in that there were five panels

over the first 10% of the chord and 12 panels over the last 90% of the chord. The wing was divided into six panels in the spanwise direction. This three-dimensional wing is shown in Figure 2.2.

When the number of panels in the spanwise direction was increased to 12, there was very little difference in the pressure coefficients as can be seen in Figure 2.3. Therefore, in the interest of minimizing computer run time, the calculations were completed with only six panels in the spanwise direction.

Experimental data was obtained for a wing based on the NACA 4412 airfoil with an aspect ratio of six (7). This wing was modeled with PMARC in the NASA Ames 12 foot wind tunnel and in the free air. The results of these calculations are shown in Figure 2.4.

For this calculation, PMARC tended to under-predict the pressure coefficient over the wing. However, the wall interference is apparent in Figure 2.4 when the free air case and the wind tunnel case are compared. A closed wall tunnel will serve to increase the angle of attack experienced by the model (10) and also increase the free stream velocity around the model. This effect appears in Figure 2.4 as an increased area between the upper and lower surface curves from the free air case to the wind tunnel case.

The experimental data used in Figure 2.4 were from a test in which the effective angle of attack, i. e. the corresponding angle for two-dimensional flow α_0, was -0.5° (7). Therefore, another calculation was performed by setting the wing modeled with PMARC at an angle of attack of -0.5° in free air. The aspect ratio was increased to 20 to better approximate two-dimensional flow. The results of this calculation as compared with the experimental data are shown in Figure 2.5. The upper surface pressure coefficients for the PMARC calculated case were approximately 13% larger than the experimental data near the quarter chord point. This difference is probably due to viscous effects (i.e. boundary layer effects) that appear in the experimental data. Since PMARC is a potential code, it can only model inviscid flow. The lower surface pressure coefficients agree well with the experimental data.

The calculations described in this section produced results that were in reasonably good agreement with previously published data. The two-dimensional wing results obtained with PMARC over the lower surface agreed well with the results obtained by Ashby and Sandlin (8) who used VSAERO. There was approximately a 12% difference over the upper surface from about 20% of the chord to 40% of the chord which was attributed to a difference in the solid blockage for the two investigations. The three-dimensional wing results obtained with PMARC, when compared with actual experimental data as obtained by Pinkerton (7), proved to be valid. Again, the lower surface data was in good agreement with Pinkerton's (7) results, but there was a 13% difference in the data on the upper surface. This difference is probably due to viscous effects in the experimental data.

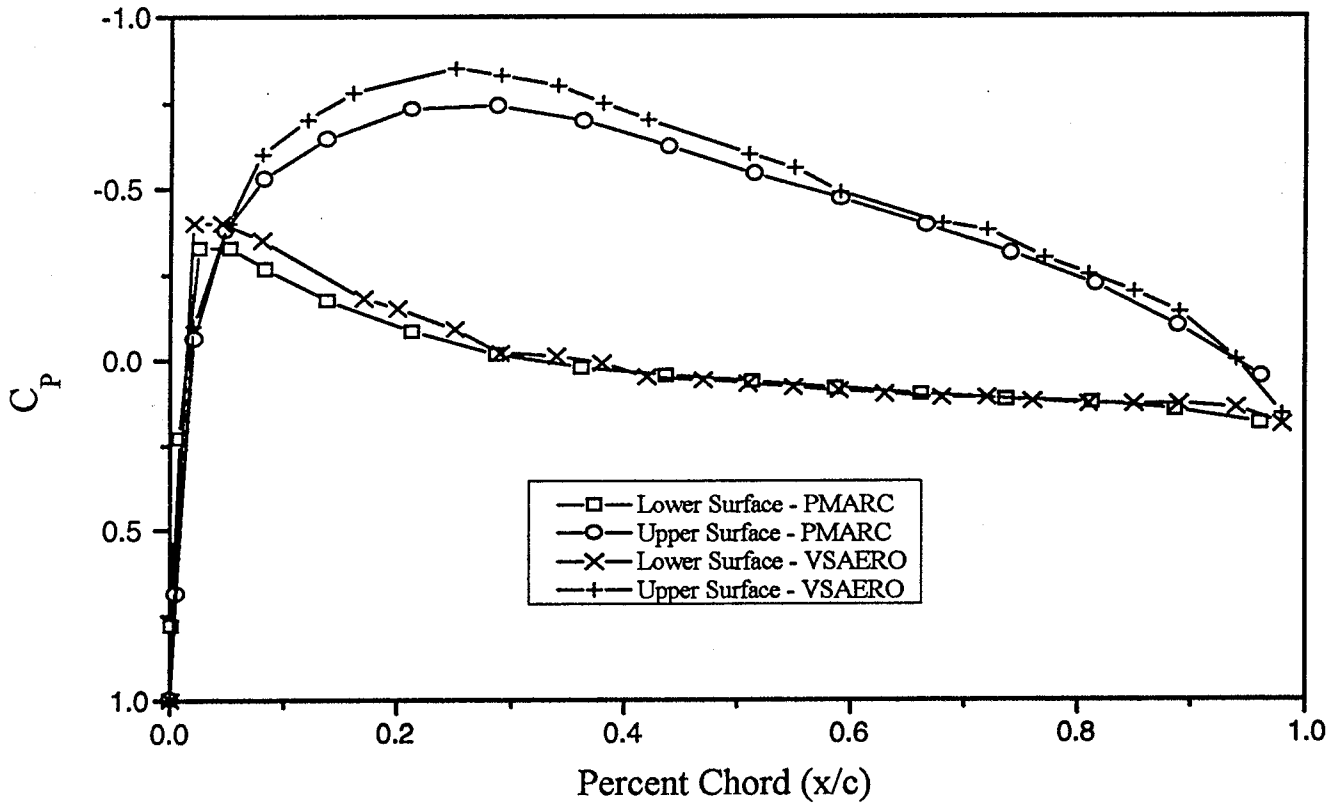

Figure 2.1. Two-dimensional airfoil pressure coefficients

Source: Ashby, D.L., Sandlin, D. R.; "Application of a Low Order Panel Method to Complex Three-Dimensional Internal Flow Problems," NASA CR-177424, 1986.

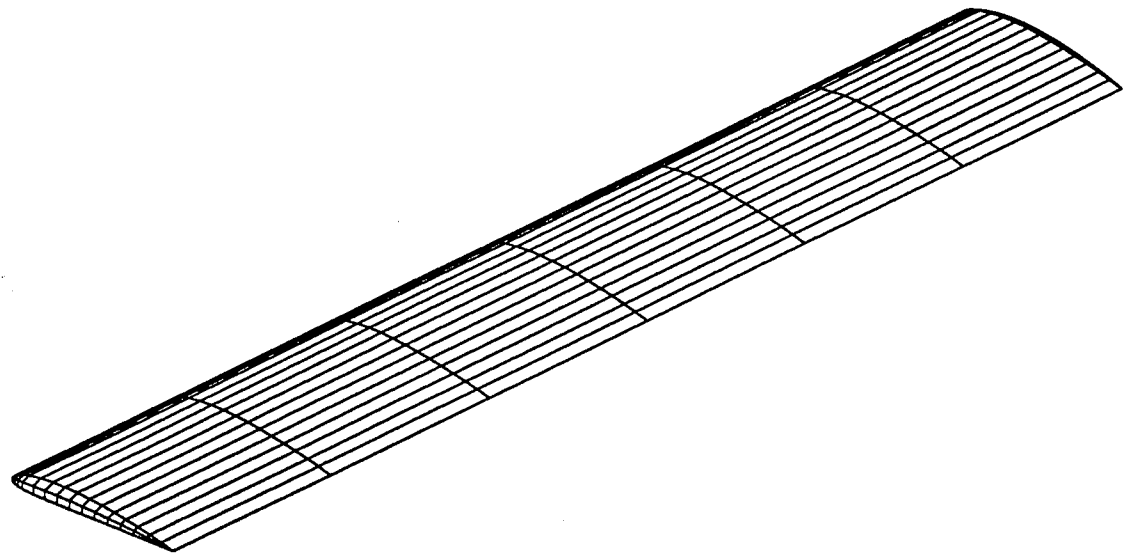

Figure 2.2. Three-dimensional wing based on the NACA 4412 airfoil

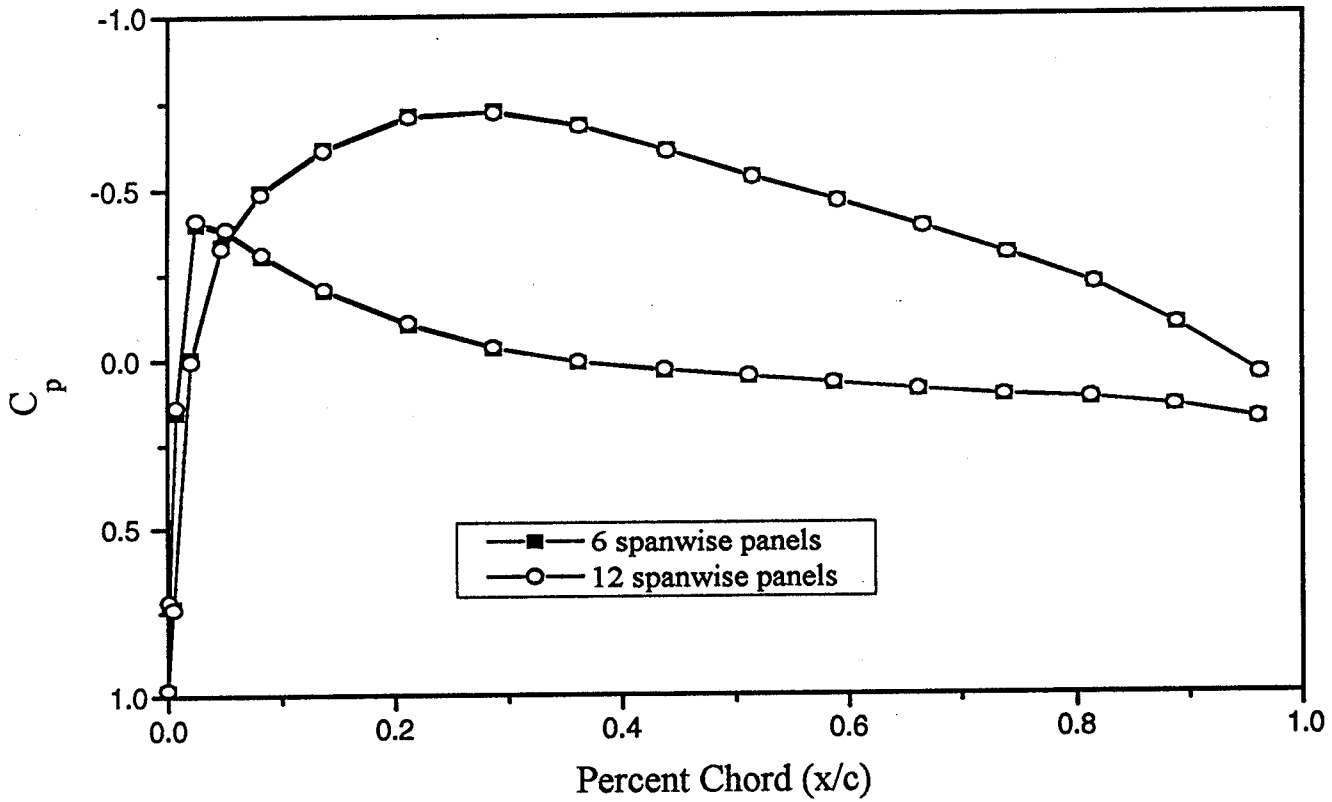

Figure 2.3. Spanwise panel distribution comparison for the three-dimensional wing

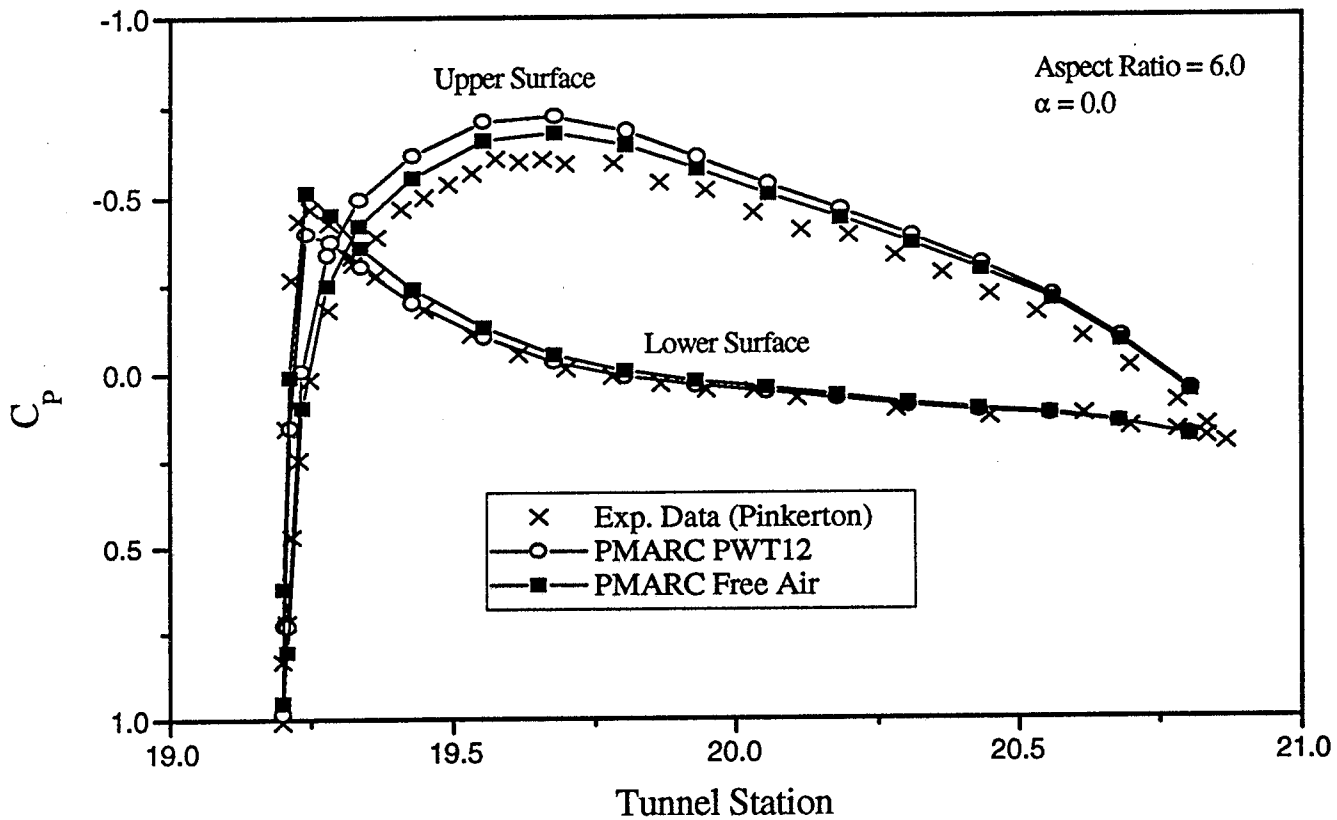

Figure 2.4. Three-dimensional wing pressure coefficients

Source: "Pinkerton, R. M.; "Calculated and Measured Pressure Distributions Over the Midspan Section of the NACA 4412 Airfoil," NACA Report 563, 1936.

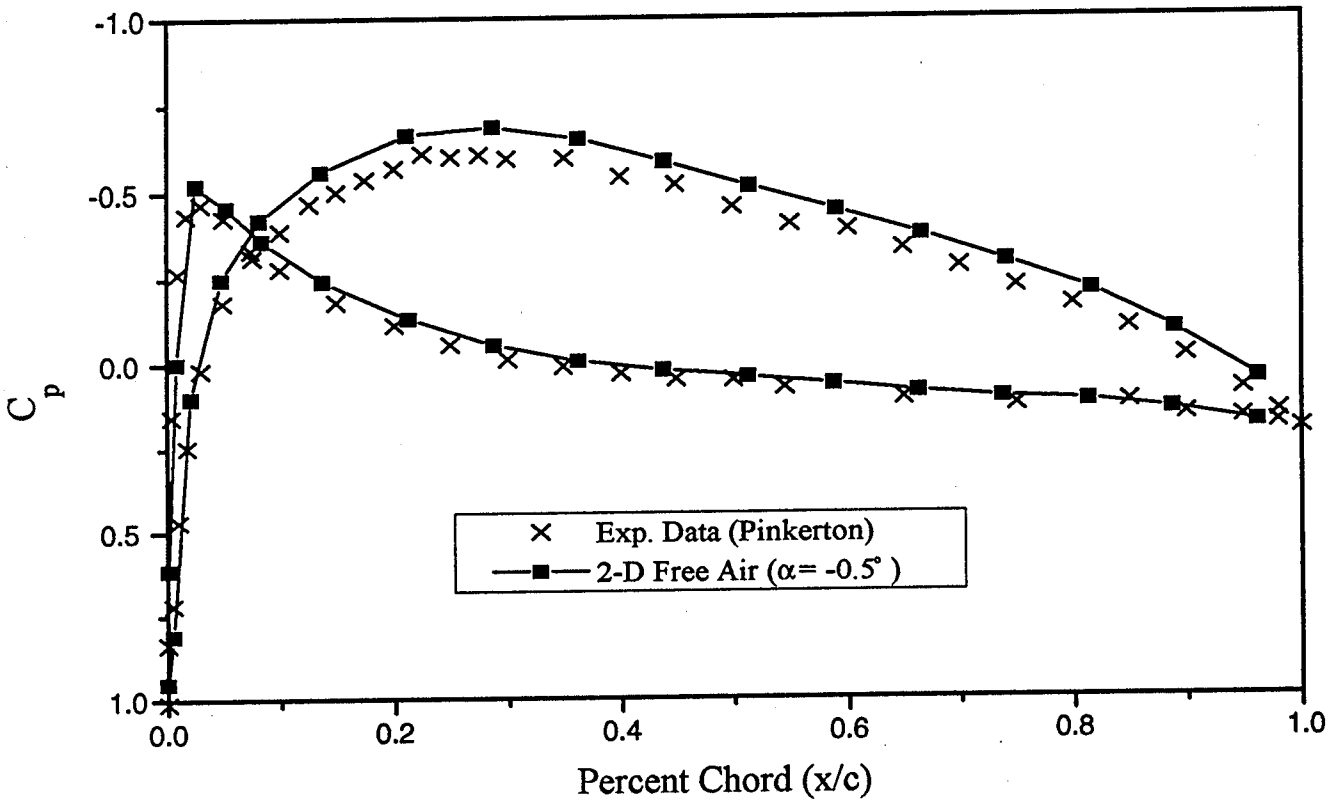

Figure 2.5. Three-dimensional wing pressure coefficients at $\alpha_0 = -0.5°$

Source: "Pinkerton, R. M.; "Calculated and Measured Pressure Distributions Over the Midspan Section of the NACA 4412 Airfoil," NACA Report 563, 1936.

3.0 Support System Interferences

This section presents the geometry description of the various components, such as the wind tunnel and the support systems, and the results of the investigation to determine the support system interference on the wall pressure in the wind tunnel. The onset flow velocity, i.e. the flow through the inlet, was set to 1.0 for all of the cases run for this investigation. All velocities were nondimensionalized by this onset flow velocity.

3.1 Description of Geometry

This investigation involved several components, each of which had to be modeled with PMARC. These components included: the wind tunnel, the strut and sting, the wing-body model, and the bi-pod support. The geometry of each of these components is described in the following sections.

3.1.1 Wind Tunnel

The twelve foot pressure wind tunnel was modeled using the machine drawings provided by NASA Ames Research Center. The cross section of the tunnel test section was basically a circle with flat walls at the top, bottom, and sides. The tunnel used in the PMARC calculations began at station 0 (101 in the drawings) and ended at station 40 (141 in the drawings). The model center was approximately located at station 20. The tunnel was modeled with a constant cross-sectional area up to station 30. At this point, the tunnel diverged to station 40. The radius to the curved portion of the wall up to station 30 was 6.0 ft. The radius to the curved wall at station 40 was 6.46 ft.

Both the inlet and exit patches consisted of 96 panels. The tunnel walls from station 0 to station 15 contained approximately 400 panels, from station 15 to station 30 contained approximately 700 panels, and from station 30 to station 40 contained approximately 500 panels. These numbers are approximate because the panel arrangement was adjusted to accommodate the support attachments to the floor and/or ceiling of the tunnel. The panels were more concentrated around the model position and around the diverging portion of the tunnel to decrease the amount of leakage caused by the flow disruption due to the model and support system. The tunnel and exit as modeled are shown in Figure 3.1.

3.1.2 Strut and Sting

The strut began at station 30 and extended downstream to station 37.6. The support extended vertically across the height of the tunnel. The strut was modeled as a symmetric airfoil according to the machine drawings.

The sting attachment was placed at the tunnel centerline for these runs. The sting could not be modeled exactly due to the fact that PMARC is a potential (and thus inviscid) code that cannot account for flow perpendicular to a surface unless the flow is allowed to pass through the surface. Also, the solution would not converge (to the 0.0005 criteria as recommended in the PMARC manual (6)) if the sting was modeled with a sharply inclined

surface. This was again attributed to the fact that such a flow requires viscous effects to describe properly. Typically, the sting should be designed such that there is a parallel section immediately aft of the model attachment point at least four sting diameters long (11). Such an arrangement, however, also produced convergence problems with PMARC. Therefore, the sting used in the calculations is an approximation of a sting that would normally be used for such a test.

The diameter of the sting at the model attachment was 0.15 ft. Nine inches downstream of the model attachment, the diameter of the sting was 0.26 ft. From this point to the strut attachment, the sting cross section changed from circular to hexagonal to match the cross section of the sting attachment.

The sting was made up of 140 panels. The strut and the sting attachment each consisted of 200 panels. This complete strut and sting assembly is shown in Figure 3.2.

3.1.3 Test Article

The test article used for these runs was the symmetric wing-body model used in the example input file in the PMARC manual (6). This model consisted of a swept wing based on a symmetric airfoil and a circular cross-section fuselage with a fineness ratio of 12 (6). The model was scaled down to have an overall length of about 6 ft. Figure 3.3 shows the wing-body model as used for this investigation. The blockage due to this model is approximately 0.4%. The aft fuselage has been cut for the sting attachment. The model surface was divided into 1,360 panels.

Figure 3.4 shows the test assembly including the wing-body model, the sting and strut, the inlet, and the exit as used in the calculations. The wind tunnel walls have been omitted for clarity.

3.1.4 Bi-pod Support

The second support investigated in this study was the bi-pod support. This support consists of two cylinders attached perpendicularly to the floor of the tunnel. From the preliminary drawings available, there did not appear to be a cowling around the cylinders. Therefore, the support was modeled simply as two cylinders extending from the floor of the wind tunnel to approximately the tunnel centerline. Figure 3.5 shows the bi-pod support geometry. The bi-pod surface consisted of a total of 280 panels.

3.2 Transition from Test Section to Diffuser

The pressure coefficients calculated along the wall at a 45° angle from the horizontal (along the curved portion of the wall) were used due to the fact that the flat walls in the actual wind tunnel have windows at which pressure measurements cannot be made. A spike was expected at the point at which the tunnel walls begin to diverge, since inviscid theory predicts that the velocity at a corner, Figure 3.6, will increase.

The velocity potential for inviscid flow around such a corner is given by Streeter (12) as

$$\phi = Ar^{\pi/\alpha} \cos\frac{\pi\theta}{\alpha} \tag{3.1}$$

from which the radial and angular velocity components around the corner are, respectively,

$$v_r = \frac{\partial\phi}{\partial r} = A\frac{\pi}{\alpha} r^{\left(\frac{\pi}{\alpha}-1\right)} \cos\frac{\pi\theta}{\alpha} \tag{3.2}$$

and

$$v_\theta = \frac{1}{r}\frac{\partial\phi}{\partial\theta} = -\frac{\pi}{\alpha} Ar^{\left(\frac{\pi}{\alpha}-1\right)} \sin\frac{\pi\theta}{\alpha}. \tag{3.3}$$

The boundary condition of no flow through the wall is satisfied, since $v_\theta = 0$ when $\theta = 0$ or $\theta = \alpha$. The angle α was found to be 1.0105π radians. The constant, A, was determined by selecting a point upstream of the corner at which the velocity was approximately V_∞ (from the PMARC output along the wall), setting this equal to v_r (since v_θ must be zero at the wall), and solving for the constant A, which was found to be 1.02393. These equations are only applicable near the corner since, as $r \to \infty$, v_r goes to zero.

Once the PMARC calculated pressure coefficients were plotted, the expected spike did appear, Figure 3.7, near the diffuser entrance. Figure 3.8 shows a comparison of the PMARC calculated velocity spike and the inviscid solution. There is good agreement between these two results near the corner.

Figures 3.7 and 3.8 illustrate the effect of corner flow on the wall pressures and velocities as calculated by PMARC. This spike appears in all of the results which show wall pressures at the diffuser entrance. The size of the spike changes slightly due to the different panel arrangements on the walls of the wind tunnel.

3.3 Strut

Once the strut was placed in the tunnel without the sting attachment, the pressure coefficients along the walls were again calculated. Since the strut blocks the tunnel and causes the velocity to increase around the strut, the pressure coefficients near the strut should be lower (more negative) than the empty tunnel pressure coefficients at the same points. This was the result when the empty tunnel case was compared to the case with the strut in the tunnel, Figure 3.9. The pressure coefficients along the wall were almost identical until approximately station 25 where the influence of the strut began to appear.

Near the end of the strut, approximately station 38, the two curves begin to converge once again.

3.4 Wing-Body

Results were calculated for the wing-body alone in the tunnel and for the wing-body model with the sting and strut as would be the case in an actual test. Since the wing-body was relatively small, the influence at the wall was expected to be negligible compared to the strut and sting influence. Figure 3.10 shows the pressure coefficients as calculated along the wall of the tunnel for the empty tunnel, the tunnel with the wing-body alone, and the tunnel with the complete test assembly.

As expected, in Figure 3.10, the curve representing the empty tunnel matches the curve representing the tunnel with the wing-body. The model was too small to produce a noticeable effect on the wall pressures. The peaks of these two curves do not match exactly due to the fact that the panels were distributed differently for these two cases. Again, the influence of the strut on the wall pressure is minimal at the model position.

Figures 3.11 and 3.12 present the pressure coefficients as calculated along the wing surface and fuselage surface, respectively, of the wing-body model with and without the sting and strut. As can be seen in Figure 3.11, the sting tends to slightly increase the pressure coefficient on the upper surface of the wing. This data was calculated at a point on the upper surface approximately one foot from the centerline of the body.

From Figure 3.12, it is apparent that the sting has the same effect on the fuselage pressure coefficient as it had on the wing, i.e., it tends to increase (more positive) the pressure coefficient on the surface of the fuselage. As stated previously, the sting modeled in this investigation did not have a constant diameter section behind the model. It has been shown by Tunnell (13) that as the constant diameter portion of the sting immediately following the model is shortened, the base pressure increases. This would result in a corresponding increase in the pressure coefficient on the aft portion of the fuselage as can be seen in Figure 3.12. This data was calculated along the centerline of the fuselage.

The size of the wing-body was then doubled in order to determine if the sting and strut had a measurable effect on the pressure at the wall with a larger model. In order to keep the model center at station 20, the sting was shortened to approximately 4 feet. The results of this calculation are shown in Figure 3.13.

Since this model was twice as large as the first model (blockage of approximately 0.8%), the effect of the model on the wall pressures was expected to appear. This effect is evident in Figure 3.13 as a hump in the pressure curve near the model position. The strut and sting effects only appear at the end of the model which would be expected due to the sting attachment. Other than this interference, the strut and sting does not have a significant effect on the wall pressure signature near the model position.

3.5 Bi-Pod Support

Once the bi-pod support was placed in the tunnel, the question of how to define the wake arose. Since the support consists of two cylinders aligned in the flow direction, the wake from the front cylinder would have a significant effect on the flow around the rear cylinder. The effect of a wake on the wall pressure coefficients for this case was unknown. Therefore, two cases were run; one case with a wake defined from the front cylinder to the rear cylinder and from the rear cylinder to a point downstream and another case without a wake. Figure 3.14 shows the wall pressure coefficients for each case. Whether or not a wake is defined has little effect on the pressure coefficients as calculated at the wall.

Figure 3.15 is a comparison of the empty tunnel wall pressures with the tunnel and bi-pod support wall pressures. The bi-pod support did cause a noticeable disturbance on the wall pressures near its position. Since the bi-pod is located at the model position, the effect of its presence in the flow field must be accounted for in any tests run with this support. A model was not used in conjunction with the bi-pod support for this investigation.

It is apparent that the strut and sting support does not significantly influence the wall pressures near the model position. However, as the model size is increased and the sting is shortened, the influence of this support on the wall pressures near the rear of the model become more pronounced. The bi-pod support alone in the tunnel does have a noticeable effect on the wall pressures near the model position due to the fact that this support is located directly under the model.

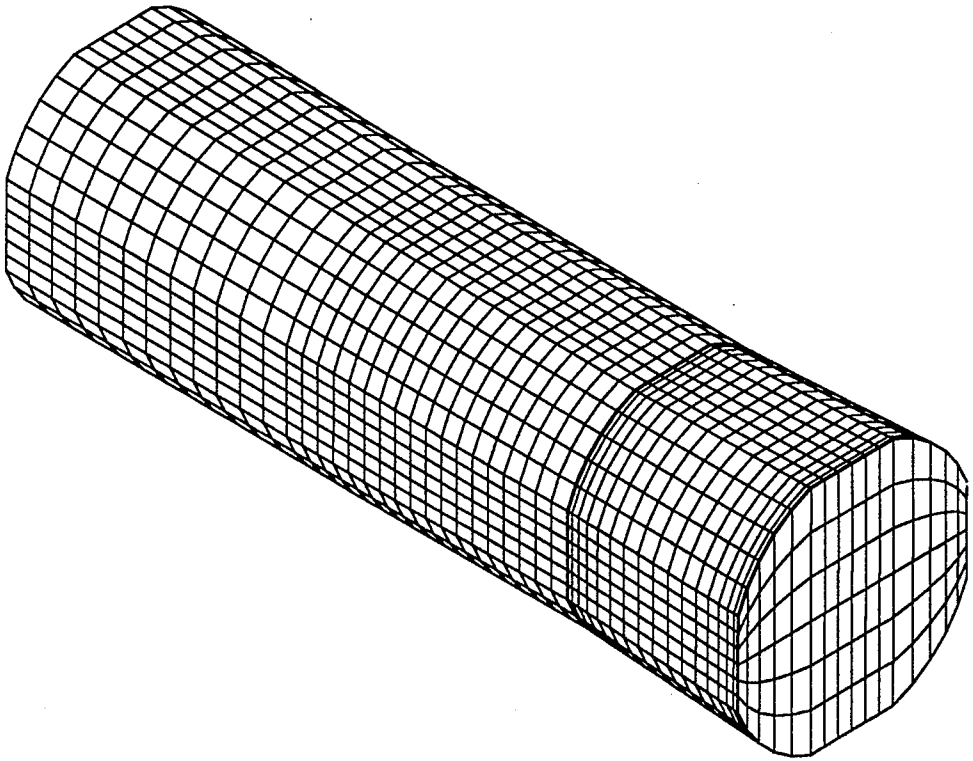

Figure 3.1. NASA Ames PWT-12 ft.

Figure 3.2. Strut and sting support

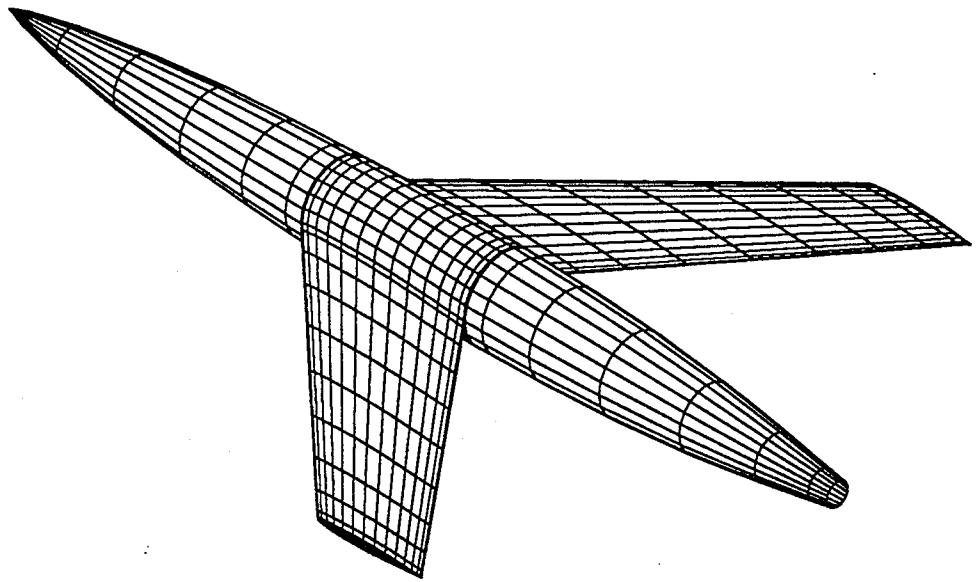

Figure 3.3. Wing-body model

Figure 3.4. Test assembly

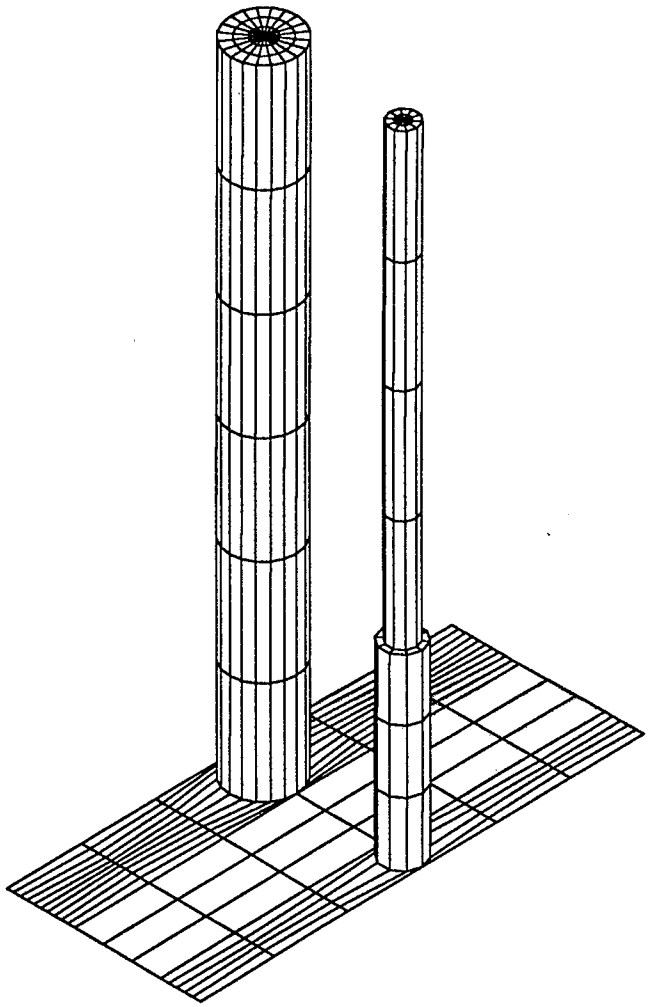

Figure 3.5. Bi-pod support

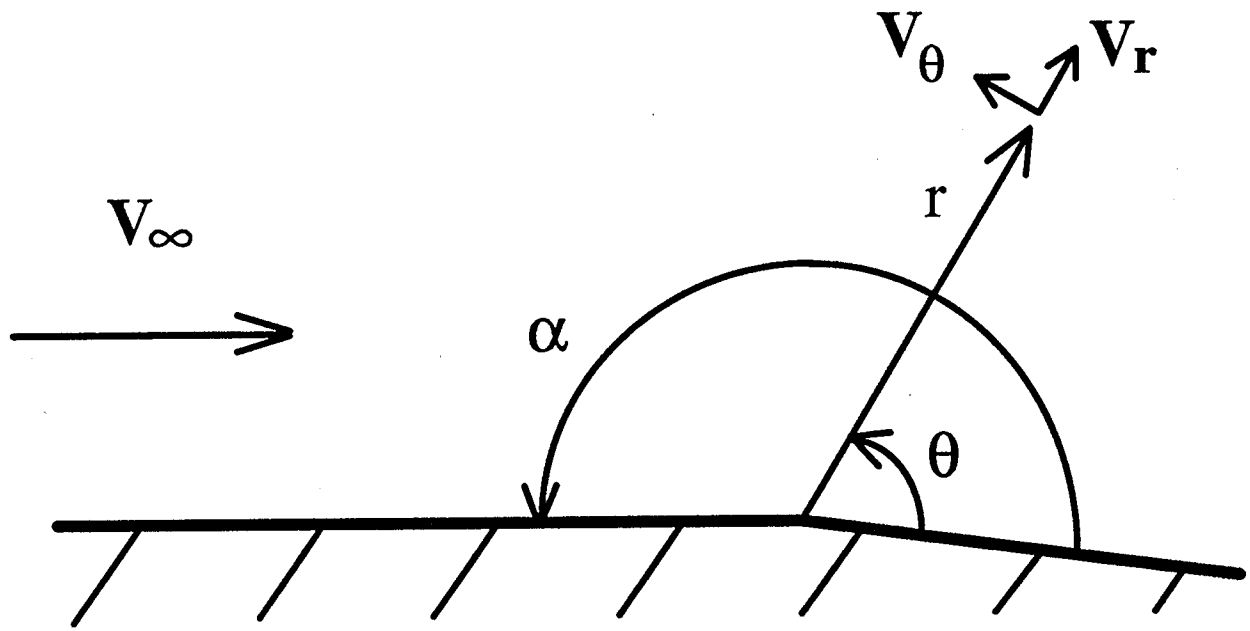

Figure 3.6. Flow around a corner

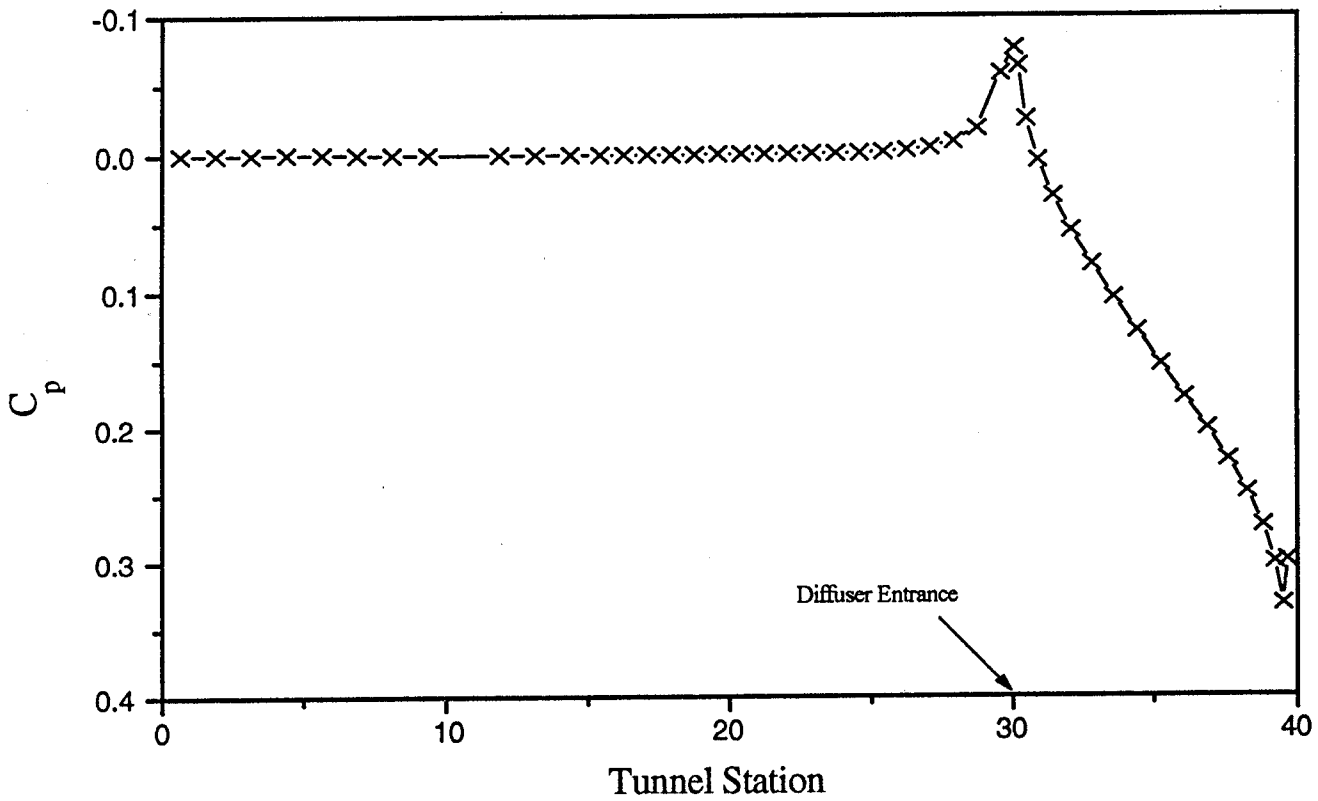

Figure 3.7. Wall pressure coefficients in the pressure wind tunnel

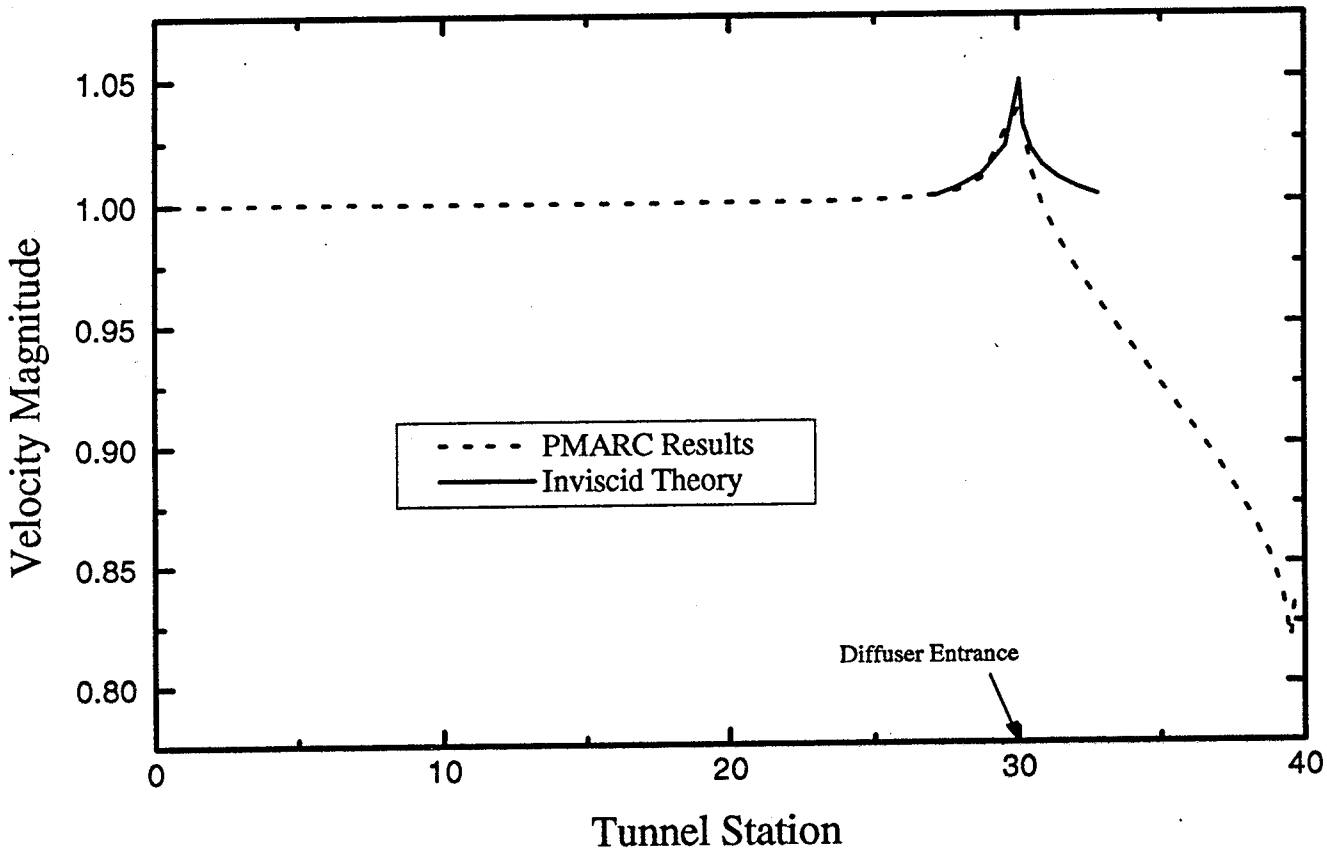

Figure 3.8. Comparison of PMARC calculated wall velocities and inviscid theory

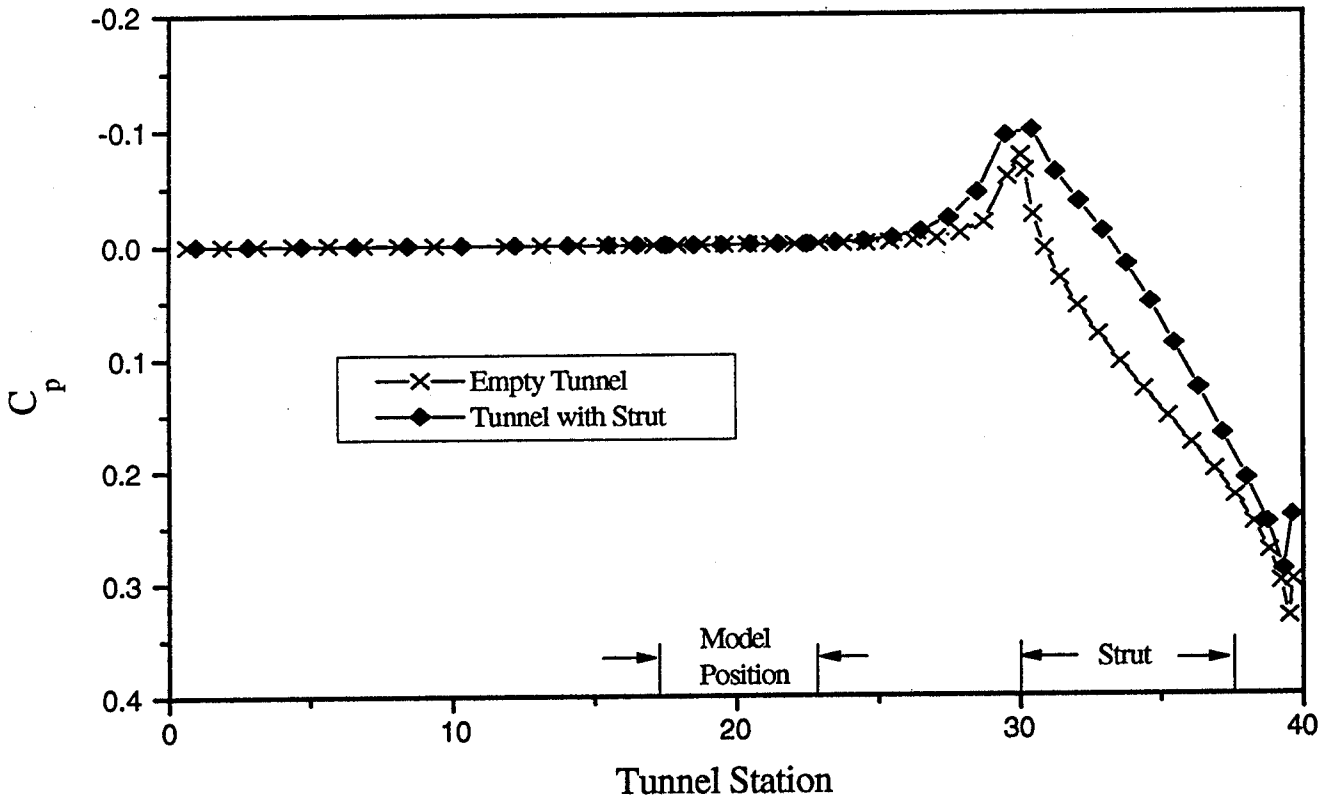

Figure 3.9. Comparison of wall pressure coefficients

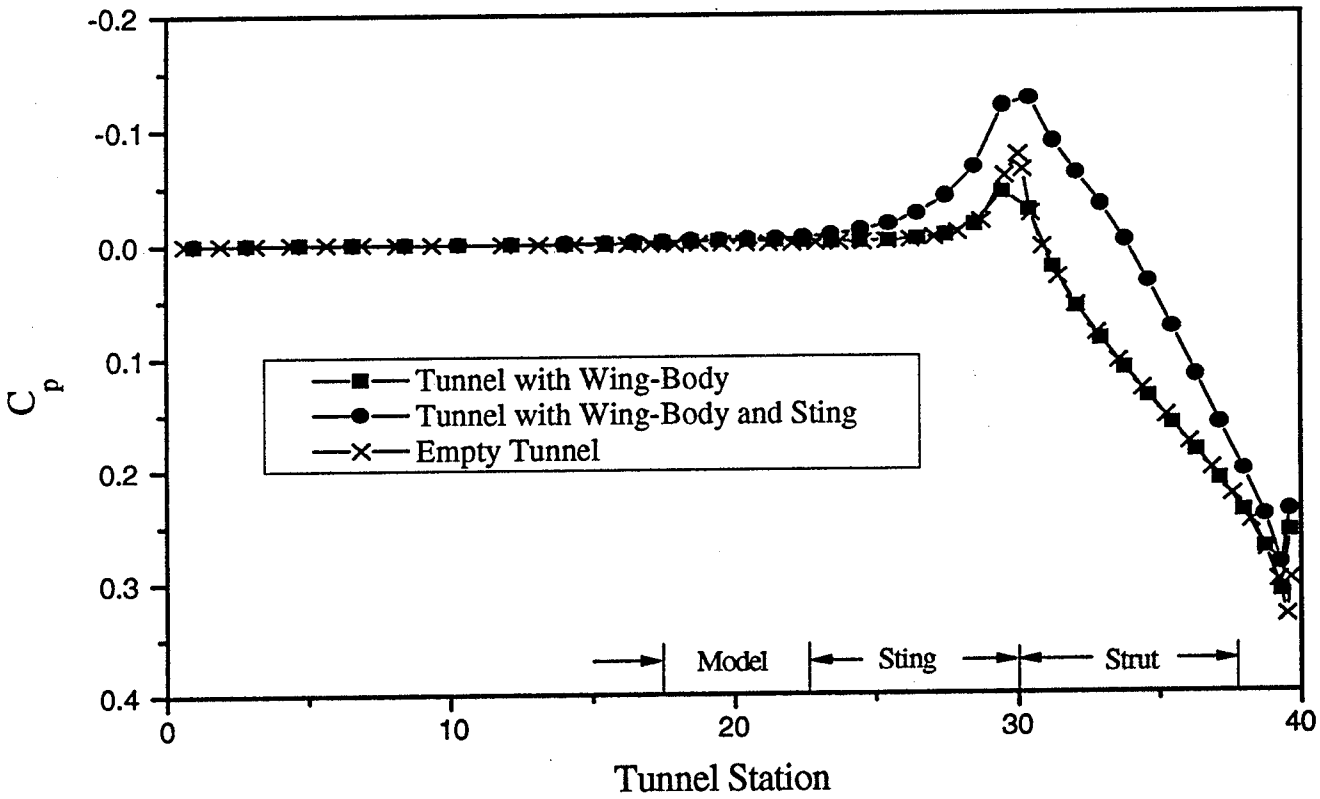

Figure 3.10. Wing-body and sting effect on wall pressure coefficients

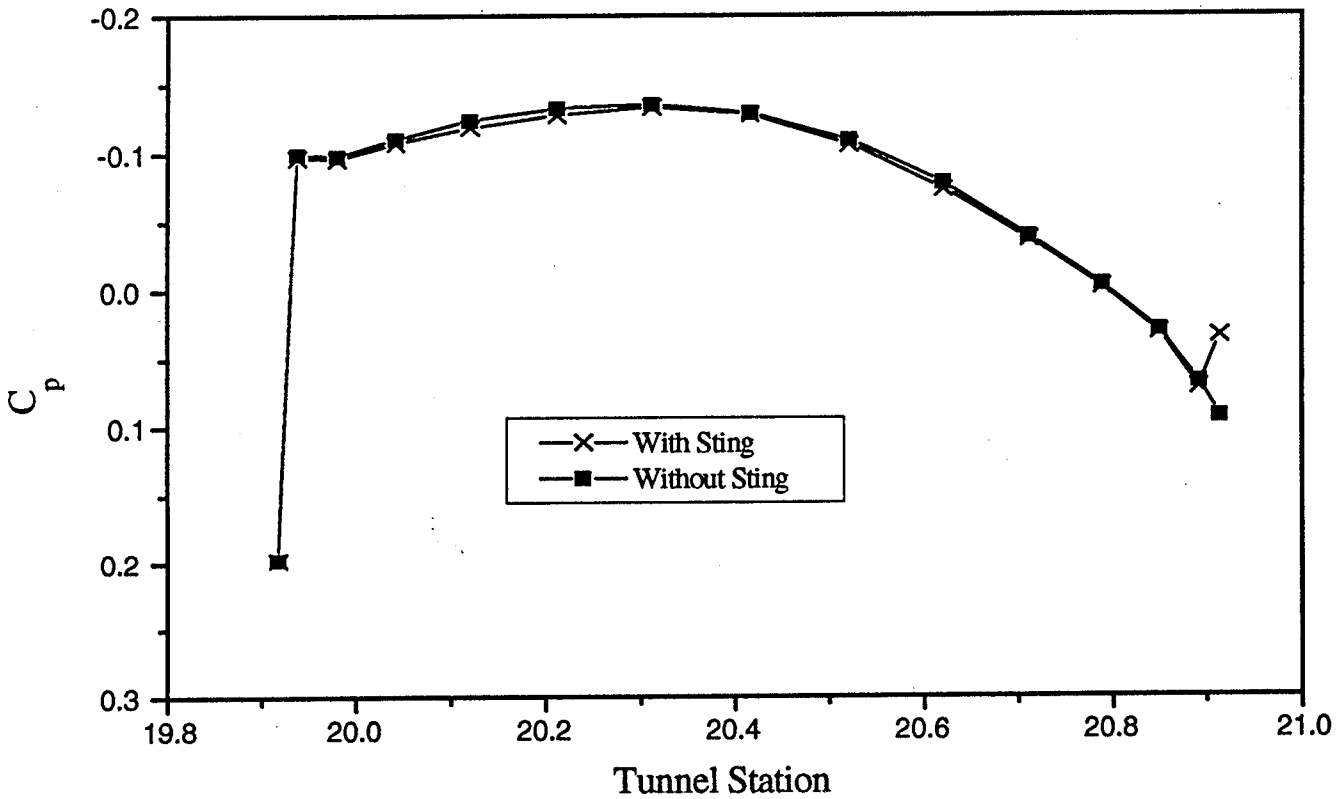

Figure 3.11. Wing upper surface pressure coefficients

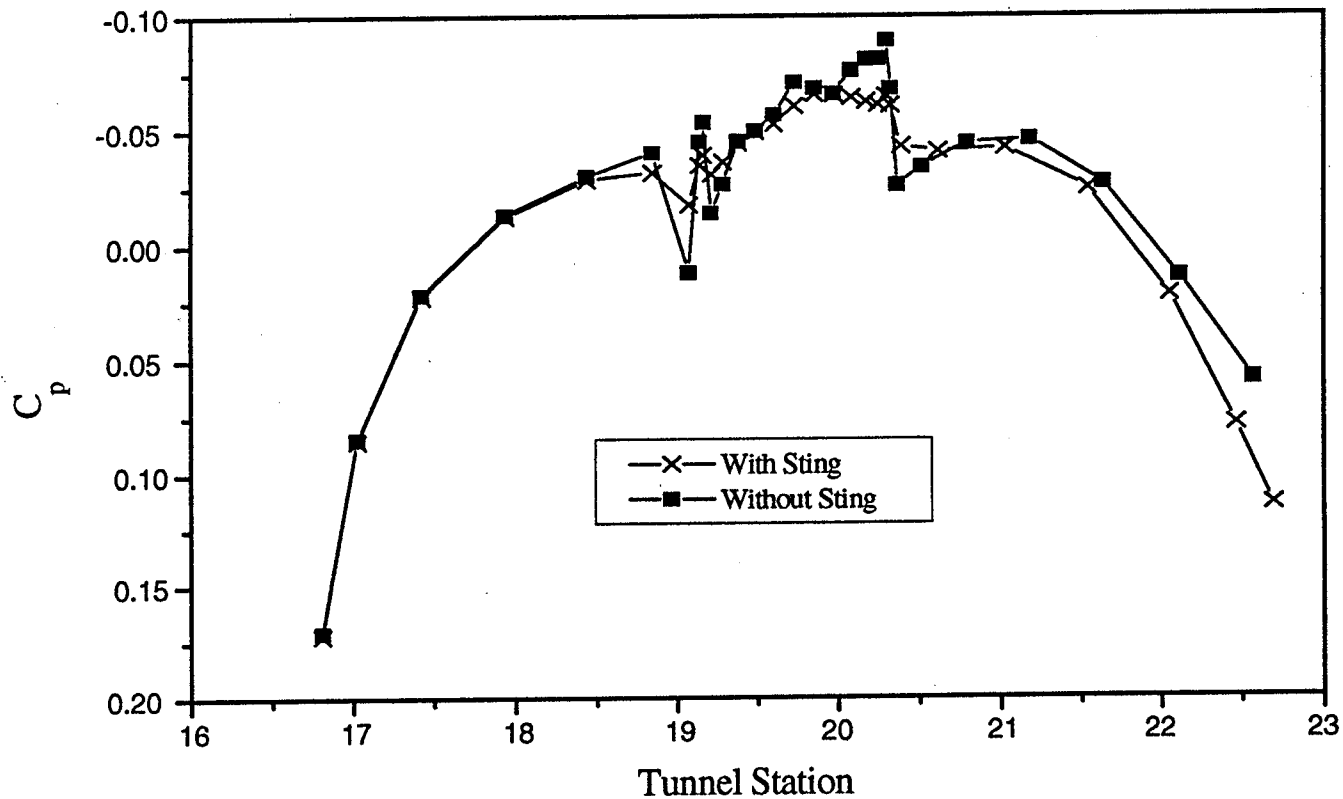

Figure 3.12. Fuselage surface pressure coefficients

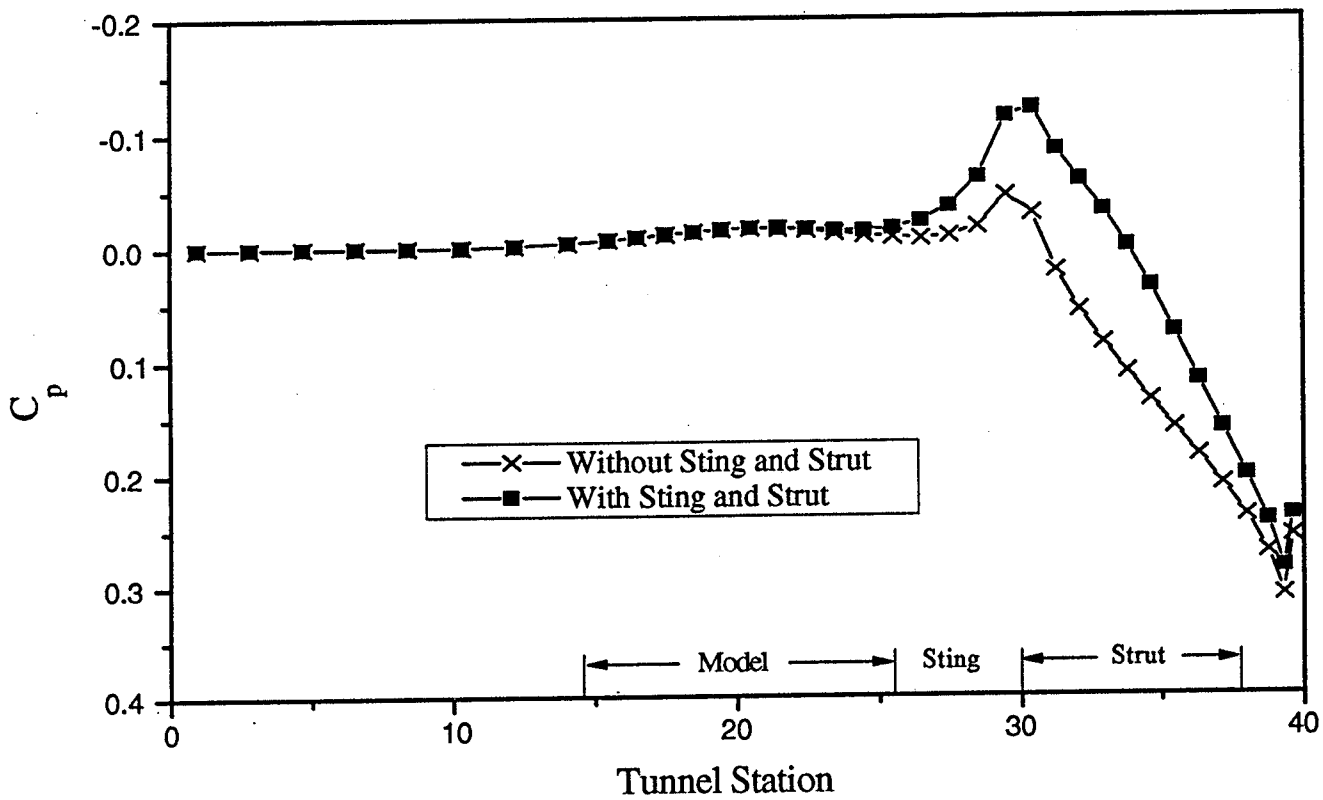

Figure 3.13. Large model effect on the wall pressure coefficients

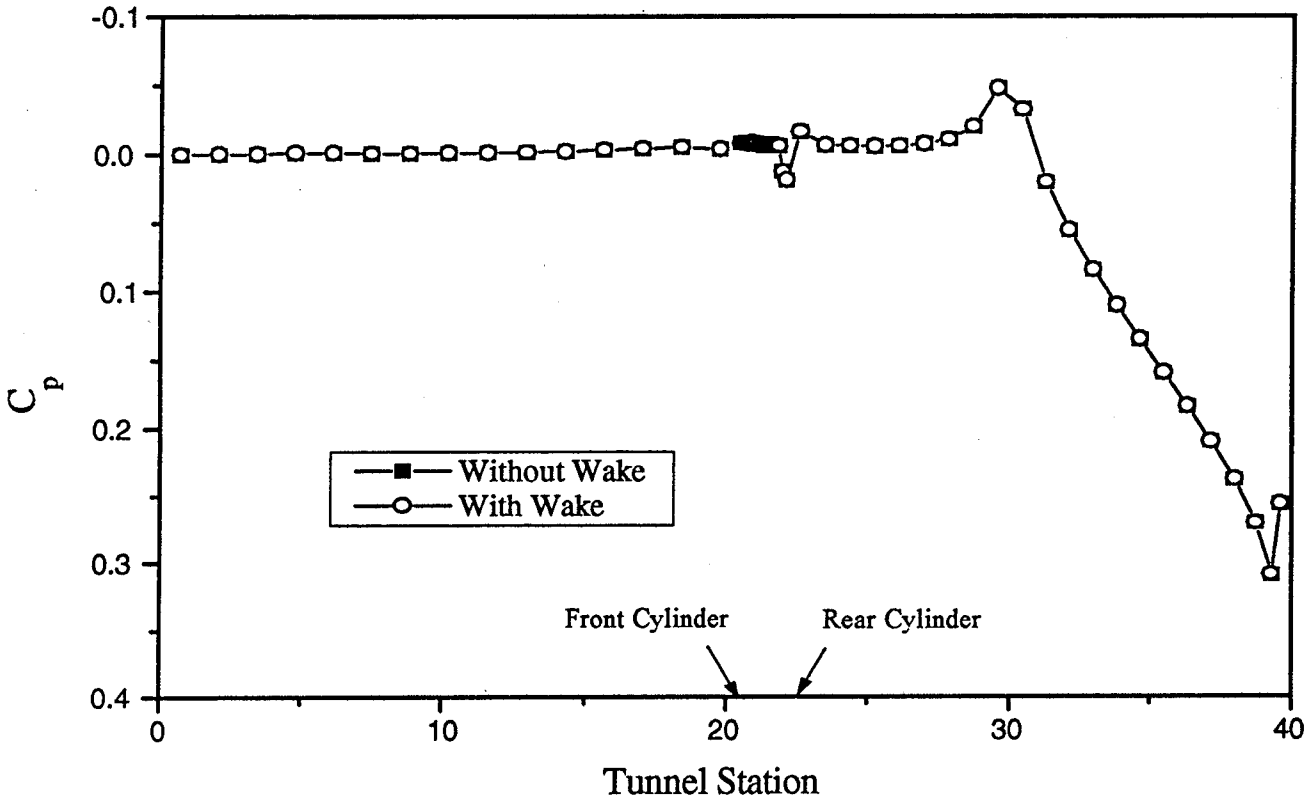

Figure 3.14. Bi-pod wake effect on wall pressure coefficients

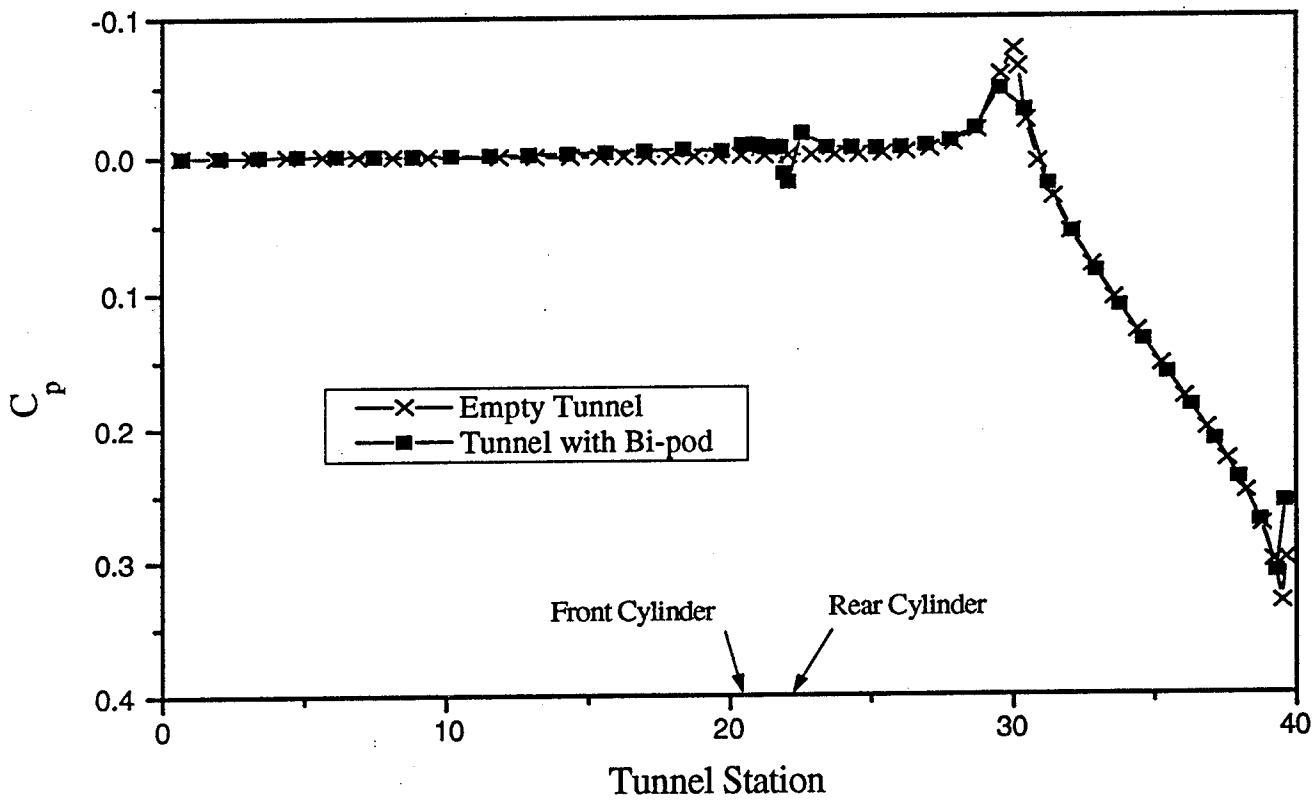

Figure 3.15. Bi-pod support effect on wall pressure coefficients

4.0 Concluding Remarks

This study has been conducted in order to determine the support system interference on the wall pressures in the NASA Ames 12 foot pressure wind tunnel. A panel method code, PMARC, was used to determine if the support system, consisting of a strut and sting and a bi-pod type support, influenced the static pressure measurements at the wall of the tunnel near the model position.

The NACA 4412 airfoil was used to examine the accuracy of the code. Both two-dimensional and three-dimensional calculations were performed and compared with published results. The results from this test agreed well with published data obtained both with another panel code and from actual experiments. Inviscid theory was used to explain a velocity spike encountered at the entrance to the diffuser.

This investigation has shown that the sting and strut support does not influence the static pressures measured along the wall around the model location. The calculations were performed for two different sizes of a model and the results were that, even with a large model, this support did not significantly influence the wall static pressures near the model. The bi-pod support was shown to have a larger influence on the wall static pressures due to the fact that it is located directly under the model. A model was not used in conjunction with the bi-pod support.

The results of this investigation can be used by the personnel at NASA Ames to show that the strut and sting support will not influence the wall static pressure measurements used to make corrections for this tunnel. However, the bi-pod support can be expected to influence the wall pressures near the model. This must be taken into account in any test performed with this support. This investigation also provides NASA Ames with a baseline for the calibration of the wind tunnel when it becomes operational.

The strut and sting support is constructed so that the vertical position of the model can be varied. The effect of this variation should be investigated to determine the influence of the sting on the wall static pressures as it approaches the floor or ceiling of the tunnel. Also, the bi-pod support should be used in conjunction with a model and the results compared to those of this investigation.

Once the wind tunnel is operational, it would be useful to compare actual experimental data taken in the tunnel with the results of this investigation. This would help to make any fine adjustments that would be needed for future study of this tunnel with PMARC.

References

1. Hackett, J. E., Wilsden, D. J.; "Determination of Low Speed Wake Blockage Corrections Via Tunnel Wall Static Pressure Measurements," AGARD CP 174, Paper 22, October 1975.

2. Kemp, W. B., Jr.; "Transonic Assessment of Two-Dimensional Wind Tunnel Wall Interference Using Measured Wall Pressures," NASA CP 2045, March 1978.

3. Ashill, P. R., Weeks, D. J.; "A Method for Determining Wall-Interference Corrections in Solid-Wall Tunnels from Measurements of Static Pressure at the Walls," AGARD CP 335, Paper 1, May 1982.

4. Ulbrich, N., Lo, C. F., Steinle, F. W.; "Blockage Correction in Three-Dimensional Wind Tunnel Testing Based on the Wall Signature Method," AIAA Paper 92-3925, Presented at the 17th Aerospace Ground Testing Conference, Nashville, TN, July 1992.

5. Lo, C. F.; "Tunnel Interference Assessment by Boundary Measurements," AIAA Journal, Vol. 16, No. 4, April 1978, pp. 411-413.

6. Ashby, D. L., Dudley, M. R., Iguchi, S. K., Browne, L., Katz, J.; "Potential Flow Theory and Operation Guide for the Panel Code PMARC," Release version 12.03 of PMARC, July 1991.

7. Pinkerton, R. M.; "Calculated and Measured Pressure Distributions Over the Midspan Section of the NACA 4412 Airfoil," NACA Report 563, 1936.

8. Ashby, D. L., Sandlin, D. R.; "Application of a Low Order Panel Method to Complex Three-Dimensional Internal Flow Problems," NASA CR-177424, 1986.

9. Loving, D. L., Estabrooks, B. B.; "Analysis of Pressure Distribution of Wing-Fuselage Configuration Having a Wing of 45° Sweepback, Aspect Ratio 4, Taper Ratio 0.6, and NACA 65A006 Airfoil Section," NACA RM L51F07, September 1951.

10. Rae, W. H., Jr., Pope, A.; *Low-Speed Wind Tunnel Testing*, 2nd Edition, John Wiley & Sons, New York, 1984.

11. Holt, D. R., Hunt, B.; "The Use of Panel Methods for the Evaluation of Subsonic Wall Interference," AGARD-CP-335, London, England, May 1982.

12. Streeter, V. L.; *Fluid Dynamics*, McGraw-Hill Publications in Aeronautical Science, McGraw-Hill Book Company, New York, 1948.

13. Tunnell, P. J.; "An Investigation of Sting-Support Interference on Base Pressure and Forebody Force at Mach Numbers from 0.60 to 1.30," NACA RM A54K16a, 1955.